East European Journal of Physics. 1. 85–94 (2024)
DOI: 10.26565/2312-4334-2024-1-06 ISSN 2312-4334

COSMIC ASPECTS OF SHARMA-MITTAL HOLOGRAPHIC DARK ENERGY MODEL IN BRANS-DICKE THEORY OF GRAVITY

Y. Aditya[a,*], D. Tejeswararao[a], U.Y. Divya Prasanthi[b]
[a] *Department of Basic Science and Humanities, GMR Institute of Technology, Rajam-532127, India*
[b] *Department of Statistics & Mathematics, College of Horticulture, Dr. Y.S.R. Horticultural University, Parvathipuram-535502, India*
[*] *Corresponding Author e-mail: aditya.y@gmrit.edu.in; yaditya2@gmail.com*
Received January 1, 2024; revised January 25, 2024; accepted February 4, 2024

We investigate the cosmological scenario involving spatially homogeneous and anisotropic Bianchi type-VI_0 space-time in the context of the Sharma-Mittal holographic dark energy model within the framework of Brans-Dicke's theory of gravitation. In order to achieve this objective, the Hubble, deceleration, equation-of-state parameters have been discussed. The deceleration parameter (q) is used to measure the pace at which the expansion of the universe is accelerating. The equation-of-state parameter (ω_{smhde}) characterizes the quintessence and vacuum areas of the universe. All the parameters demonstrate consistent behaviour following the Planck 2018 data. We assess the dynamical stability by defining the squared speed of sound and examining its behaviour. In addition, the energy conditions and the variation of ω_{smhde} and ω'_{smhde} in the model indicate the present accelerating expansion of the universe.

Keywords: *Bianchi type-VI_0 model; Dark energy model; Brans-Dicke theory of gravity; Cosmology; Sharma-Mittal holographic dark energy*

PACS: 98.80.-k, 95.36.+x

1. INTRODUCTION

The phenomenon of accelerated expansion of the universe has been thoroughly demonstrated by several observations [1]-[3]. Studies imply that the universe is spatially flat and consists of two main components: dark energy (DE) with negative pressure, dust matter composed of cold dark matter (CDM) and baryons. To understand the nature of DE, it is necessary to determine whether it arises from a cosmological constant (Λ) or a dynamical model. The dynamical DE models may be distinguished from the cosmological constant by using the equation of state (EoS) parameter $\omega_{DE} = \frac{p_{DE}}{\rho_{DE}}$, where p_{DE} represents the pressure and ρ_{DE} represents the energy density of DE. Multiple possibilities for differential evolution have been suggested (Copeland et al. [4]). The data analysis of SNeIa demonstrates that these dynamical models are more consistent with the current understanding of the universe compared to Λ. An alternative approach involves altering the geometric component of the Einstein-Hilbert action, which is referred to as modified theories of gravity, to analyze the expansion phenomena. For a comprehensive examination of DE and modified theories of gravity, please refer to the sources cited as [5]-[7]. The developments in the exploration of black hole theory and string theory have led to the formulation of the holographic principle. This principle suggests that the number of possible configurations of a physical system should be limited as well as that this limitation should be determined by the system's surface area rather than its volume. Additionally, the holographic principle suggests that there should be a restriction on the system's lowest energy state.

The holographic DE (HDE) is a very intriguing dynamical concept that is founded upon the holographic principle. The validity of HDE has been evaluated and verified by many astronomical methodologies, including using the anthropic principle (Huang and Li [8]). Incorporating the holographic principle into cosmology allows for determining the maximum amount of entropy present in the universe. Li [9] put the following limit on the DE density, as stated by Cohen et al. [10]

$$\rho_{DE} = 3d^2 m_p^2 L^{-2}. \tag{1}$$

the symbol m_p represents the decreased Planck mass, $3d^2$ indicates a numerical constant, and L represents the IR-cutoff. Several types of IR-cutoff have been investigated in academic studies, including the Hubble horizon H^{-1}, event horizon, particle horizon, conformal universe age, Ricci scalar radius, and Granda–Oliveros cutoff [11]-[12]. The HDE models, using various infrared cutoffs, provide a modern understanding of the universe's acceleration. They additionally demonstrate that the transition redshift value, which marks the transfer from a previous deceleration phase (q>0) to the current acceleration phase (q<0), corresponds with contemporary

Cite as: Y. Aditya, D. Tejeswararao, U.Y.D. Prasanthi, East Eur. J. Phys. 1, 85 (2024), https://doi.org/10.26565/2312-4334-2024-1-06

observable data. Nojiri and Odintsov [13] proposed a technique to merge the initial and final phases of the universe by using generalized HDE and phantom cosmology. They have now expanded this notion to what they refer to as Hinflation [14]. Various formulations of entropy have been used in recent decades to construct and analyze cosmological models. Multiple innovative models of HDE have been developed, such as the Tsallis HDE [15, 16], the Sharma-Mittal HDE (SMHDE) [17], and the Renyi HDE model [18]. Numerous researchers have evaluated different cosmological models of new HDE models [19]- [30]. Jawad and Sultan [31], Sharma [32], and Drepanou et al. [33] have investigated SMHDE models within different gravitational theories. The researchers Sadeghi et al. [34] examined the dynamic formations of HDE within the framework of Brans-Dicke's theory of gravity, using the Tsallis and Kaniadakis methodologies.

In the last few decades, universes that are both spatially homogeneous and anisotropic have attracted a lot of attention from theoretical cosmologists. According to Akarsu and Kilinc [35], the main empirical data from CMBR (Bennett et al. [36]) supports the idea that the universe is transitioning from a non-uniform to a uniform phase. Moreover, it is believed that the isotropic FRW model may not provide a complete and correct picture of matter in the early universe. It is essential to take into account anisotropic space-times to objectively evaluate cosmological models for their ability to attain the observed degree of homogeneity and isotropy. Because of its anisotropic character, researchers have given a lot of attention to homogeneous but not necessarily isotropic Bianchi type (BT) cosmological models. In the framework of anisotropic Bianchi type space-times, several renowned researchers have recently proposed fascinating cosmological models that include DE. several researchers (Ref. [37]-[49]) have looked at anisotropic cosmological models in various scenarios.

In this work, we take into account the BT-VI_0 universe filled with matter and SMHDE within the framework of Brans-Dicke's theory of gravitation, motivated by the previously mentioned findings and discussion. This paper's work is organized in the following way: Section-2 contains the BT-VI_0 metric and field equations of the model using anisotropic SMHDE fluid and matter. In addition, we constructed the SMHDE model and found the solutions to the field equations in section-3. Various cosmological parameters that constitute our model are presented in section-4. In the last section, we derive a few conclusions based on our results.

2. METRIC AND FIELD EQUATIONS

The Brans-Dicke [50] field equations in the presence of matter and DE are given by

$$R_{ij} - \frac{1}{2}Rg_{ij} = -8\pi\phi^{-1}\left(T_{ij} + \overline{T}_{ij}\right) - w\phi^{-2}\left(\phi_{,i}\phi_{,j} - \frac{1}{2}g_{ij}\phi_{,k}\phi^{,k}\right) - \phi^{-1}\left(\phi_{i;j} - g_{ij}\phi^{;k}_{;k}\right), \tag{2}$$

and

$$\phi^{;k}_{;k} = 8\pi\left(T + \overline{T}\right)(3+2w)^{-1}.$$

Also, the energy conservation equation is

$$\left(T^{ij} + \overline{T}^{ij}\right)_{;j} = 0. \tag{3}$$

The energy-momentum tensor for the matter and DE are respectively defined as

$$\overline{T}_{ij} = \rho_m u_i u_j, \quad T_{ij} = (\rho_{smhde} + p_{smhde})u_i u_j - p_{smhde} g_{ij}. \tag{4}$$

Here ρ_m, ρ_{smhde} are the energy densities of matter and the dark energy respectively. p_{smhde} is the pressure of the dark energy. In a comoving coordinate system, from equations (4), we get

$$T^1_1 = T^2_2 = T^3_3 = -p_{smhde}, T^4_4 = \rho_{smhde} \quad ; \quad \overline{T}^1_1 = \overline{T}^2_2 = \overline{T}^3_3 = 0, \overline{T}^4_4 = \rho_m \tag{5}$$

where ρ_m, ρ_{smhde} and p_{smhde} are the functions of cosmic time t only.

We consider the geometry of the universe as spatially homogeneous and anisotropic BT-VI_0 line element which can be written as

$$ds^2 = dt^2 - A^2dx^2 - B^2e^{2x}dy^2 - C^2e^{-2x}dz^2, \tag{6}$$

where A, B and C are functions of cosmic time t only. The following are the some of physical parameters which are useful in finding the solution of field equations for the BT-VI_0 space-time given by Eq. (6). The average scale factor $a(t)$ and volume V of the BT-VI_0 space-time are defined as

$$V = [a(t)]^3 = ABC. \tag{7}$$

Anisotropic parameter A_h is given by

$$A_h = \frac{1}{3}\sum_{i=1}^{3}\left(\frac{H_i - H}{H}\right)^2 \tag{8}$$

where $H_1=\frac{\dot{A}}{A}, H_2=\frac{\dot{B}}{B}, H_3=\frac{\dot{C}}{C}$ are directional Hubble's parameters and $H=\frac{1}{3}\left(\frac{\dot{A}}{A}+\frac{\dot{B}}{B}+\frac{\dot{C}}{C}\right)$ is mean Hubble's parameter. Here and after an overhead dot denotes differentiation concerning cosmic time t. Expansion scalar (θ) and shear scalar (σ^2) are defined as

$$\theta=u^i_{;i}=\frac{\dot{A}}{A}+\frac{\dot{B}}{B}+\frac{\dot{C}}{C} \tag{9}$$

$$\sigma^2=\frac{1}{3}\left(\frac{\dot{A}^2}{A^2}+\frac{\dot{B}^2}{B}+\frac{\dot{C}^2}{C^2}-\frac{\dot{A}\dot{B}}{AB}-\frac{\dot{A}\dot{C}}{AC}-\frac{\dot{B}\dot{C}}{BC}\right) \tag{10}$$

where $u_i=(1,0,0,0)$ is the four-velocity in the comoving coordinates. The deceleration parameter is given by

$$q=\frac{d}{dt}\left(\frac{1}{H}\right)-1. \tag{11}$$

In the comoving coordinate system, with the help of (5), the field equations (2) for the metric (6) can be written as

$$\frac{\ddot{B}}{B}+\frac{\ddot{C}}{C}+\frac{\dot{B}\dot{C}}{BC}+\frac{1}{A^2}+\frac{w}{2}\frac{\dot{\phi}^2}{\phi^2}+\frac{\dot{\phi}}{\phi}\left(\frac{\dot{B}}{B}+\frac{\dot{C}}{C}\right)+\frac{\ddot{\phi}}{\phi} = -8\pi\frac{\omega_{smhde}\rho_{smhde}}{\phi} \tag{12}$$

$$\frac{\ddot{A}}{A}+\frac{\ddot{C}}{C}+\frac{\dot{A}\dot{C}}{AC}-\frac{1}{A^2}+\frac{w}{2}\frac{\dot{\phi}^2}{\phi^2}+\frac{\dot{\phi}}{\phi}\left(\frac{\dot{A}}{A}+\frac{\dot{C}}{C}\right)+\frac{\ddot{\phi}}{\phi} = -8\pi\frac{\omega_{smhde}\rho_{smhde}}{\phi} \tag{13}$$

$$\frac{\ddot{A}}{A}+\frac{\ddot{B}}{B}+\frac{\dot{A}\dot{B}}{AB}-\frac{1}{A^2}+\frac{w}{2}\frac{\dot{\phi}^2}{\phi^2}+\frac{\dot{\phi}}{\phi}\left(\frac{\dot{A}}{A}+\frac{\dot{B}}{B}\right)+\frac{\ddot{\phi}}{\phi} = -8\pi\frac{\omega_{smhde}\rho_{smhde}}{\phi} \tag{14}$$

$$\frac{\dot{A}\dot{B}}{AB}+\frac{\dot{B}\dot{C}}{BC}+\frac{\dot{A}\dot{C}}{AC}-\frac{1}{A^2}-\frac{w}{2}\frac{\dot{\phi}^2}{\phi^2}+\frac{\dot{\phi}}{\phi}\left(\frac{\dot{A}}{A}+\frac{\dot{B}}{B}+\frac{\dot{C}}{C}\right) = 8\pi\left(\frac{\rho_{smhde}+\rho_m}{\phi}\right) \tag{15}$$

$$\frac{\dot{B}}{B}-\frac{\dot{C}}{C} = 0 \tag{16}$$

$$\ddot{\phi}+\dot{\phi}\left(\frac{\dot{A}}{A}+\frac{\dot{B}}{B}+\frac{\dot{C}}{C}\right) = \frac{8\pi}{(3+2w)}(\rho_{smhde}-3p_{smhde}+\rho_m). \tag{17}$$

Also the energy conservation equation (3) can be written as

$$\dot{\rho_m}+\left(\frac{\dot{A}}{A}+\frac{\dot{B}}{B}+\frac{\dot{C}}{C}\right)(\rho_m+\rho_{smhde}+p_{smhde})+\dot{\rho}_{smhde}=0 \tag{18}$$

where an overhead dot denotes differentiation with respect to time t and EoS parameter of DE is $\omega_{smhde}=\frac{p_{smhde}}{\rho_{smhde}}$. From (16) by taking the integrating constant as unity, we get

$$C=B \tag{19}$$

Using equation (19), the field equations (12) to (17) reduce to

$$2\frac{\ddot{B}}{B}+\frac{\dot{B}^2}{B^2}+\frac{1}{A^2}+\frac{w}{2}\frac{\dot{\phi}^2}{\phi^2}+2\frac{\dot{\phi}}{\phi}\frac{\dot{B}}{B}+\frac{\ddot{\phi}}{\phi} = -8\pi\frac{\omega_{smhde}\rho_{smhde}}{\phi} \tag{20}$$

$$\frac{\ddot{A}}{A}+\frac{\ddot{B}}{B}+\frac{\dot{A}\dot{B}}{AB}-\frac{1}{A^2}+\frac{w}{2}\frac{\dot{\phi}^2}{\phi^2}+\frac{\dot{\phi}}{\phi}\left(\frac{\dot{A}}{A}+\frac{\dot{B}}{B}\right)+\frac{\ddot{\phi}}{\phi} = -8\pi\frac{\omega_{smhde}\rho_{smhde}}{\phi} \tag{21}$$

$$2\frac{\dot{A}\dot{B}}{AB}+\frac{\dot{B}^2}{B^2}-\frac{1}{A^2}-\frac{w}{2}\frac{\dot{\phi}^2}{\phi^2}+\frac{\dot{\phi}}{\phi}\left(\frac{\dot{A}}{A}+2\frac{\dot{B}}{B}\right) = 8\pi\left(\frac{\rho_{smhde}+\rho_m}{\phi}\right) \tag{22}$$

$$\ddot{\phi}+\dot{\phi}\left(\frac{\dot{A}}{A}+2\frac{\dot{B}}{B}\right)+ = \frac{8\pi}{(3+2w)}(\rho_{smhde}-3p_{smhde}+\rho_m). \tag{23}$$

3. MODEL AND COSMOLOGICAL PARAMETERS

The field equations (20)-(23) form a set of four distinct equations involving six variables: $A, B, \rho_{smhde}, \omega_{smhde}, \rho_m$, and ϕ. To get a deterministic outcome for the nonlinear field equations in our model, we impose the following reasonable physical constraints. we consider the fact that expansion scalar θ is directly proportional to shear scalar σ which leads to a relation between the metric potentials as follows

$$B{=}A^k \tag{24}$$

k represents a positive constant that accounts for the anisotropy of space-time. Collins et al. [51] have determined that in a spatially homogeneous space-time, the normal congruence to the homogeneous expansion adheres to the constraint that the ratio of the shear stress (σ) to the Hubble parameter (H) remains constant.

In addition, it is common in the literature to employ a power-law relationship between scalar field ϕ and average scale factor $a(t)$ of the form (Johri and Sudharsan [52]; Johri and Desikan [53]) $\phi \propto [a\,(t)]^n$ where n denotes a power index. Many authors have looked into different aspects of this type of scalar field ϕ. Given the physical significance of preceding relationship, we employ the following assumption to reduce the mathematical complexity of the system

$$\phi(t) = \phi_0[a(t)]^n. \tag{25}$$

Using the relations (24) and (25) in Eqs. (20) and (21), we obtain the metric potentials as

$$A(t) = \sqrt{\frac{k_2\,t^2}{4} - \frac{A_0}{k_2}};\quad B(t) = C(t) = \left(\frac{k_2\,t^2}{4} - \frac{A_0}{k_2}\right)^{\frac{k}{2}} \tag{26}$$

where $k_2 = \frac{2}{1-k}$, $n = \frac{3-6k}{2k+1}$, A_0 is an integrating constant. The scalar field of the model is

$$\phi(t) = \phi_0\left(\frac{k_2\,t^2}{4} - \frac{A_0}{k_2}\right)^{\frac{n(2k+1)}{6}}. \tag{27}$$

Now metric (6), with the help of metric potentials in Eq. (26), can be written as

$$ds^2 \;=\; dt^2 - \left(\frac{k_2\,t^2}{4} - \frac{A_0}{k_2}\right)dx^2 - \left(\frac{k_2\,t^2}{4} - \frac{A_0}{k_2}\right)^k\left(e^{2x}dy^2 + e^{-2x}dz^2\right). \tag{28}$$

Eq. (28) represents a spatially homogeneous and anisotropic BT-VI_0 SMHDE model within the framework of Brans-Dicke theory of gravitation with the following physical parameters. The average scale factor $a(t)$ and volume $V(t)$ of the model are, respectively, given by

$$V(t) = a(t)^3 = \left(\frac{k_2\,t^2}{4} - \frac{A_0}{k_2}\right)^{\frac{2k+1}{2}}. \tag{29}$$

The average Hubble's parameter H and expansion scalar θ are obtained as

$$H = 3\theta{=}(2\,k+1)\,k_2\,t\left(3\,k_2\,t^2 - 12\,\frac{A_0}{k_2}\right)^{-1}. \tag{30}$$

The shear scalar σ^2 and average anisotropic parameter A_h are given by

$$\sigma^2{=}\frac{k_2^2(k-1)^2t^2}{3\left(k_2\,t^2 - 4\,\frac{A_0}{k_2}\right)^2}\;;\quad A_h{=}\frac{2(k-1)^2}{(2k+1)^2}. \tag{31}$$

From the above parameters it is observed that both the spatial volume and average scale factor of the universe exhibit the expansion of the universe. Furthermore, during the first epoch, which is when $t{=}\,0$, all values become finite. However, as t approaches infinity, they diverge. It is worth mentioning that when $k{=}\,1$, the model becomes shear-free and isotropic, as shown by the conditions $\sigma^2{=}\,0$ and $A_h{=}\,0$.

As a dynamical DE component, we assume Sharma-Mittal holographic DE. It is defined by (Sharma and Mittal [54]) and is formulated using Sharma-two-parametric Mittal's entropy

$$S_{SM} = \frac{1}{d_1}\left(\left(1 + \frac{\delta\kappa}{4}\right)^{\frac{d_1}{\delta}} - 1\right), \tag{32}$$

where $\kappa = 4\pi L^2$ and L represents the IR cutoff. R and δ are two free parameters in this case. At the appropriate d_1 limits, Renyi and Tsallis entropies can be recovered. Sharma-Mittal entropy is transformed into Renyi entropy in the limit $d_1 \to 0$, and Tsallis entropy in the limit $d_1 \to 1-\delta$. According to Cohen et al. [10], the relationship between the system entropy and the IR and UV cutoffs yields the energy density

$$\rho_{de} = \frac{3d_2^2 S_{SM}}{8\pi L^4}. \tag{33}$$

Using the above equation and the Hubble horizon cutoff $L = \frac{1}{H}$, we can calculate the energy density of the Sharma-Mittal HDE model (Jahromi et al. [17]) as follows:

$$\rho_{de} = \frac{3d_2^2 H^4}{8\pi d_1}\left(\left(1+\frac{\delta\pi}{H^2}\right)^{\frac{d_1}{\delta}} - 1\right), \tag{34}$$

where C^2 denotes the free parameter. Using Hubble parameter $H(t)$ in the above Eq. (34), we get the energy density of SMHDE of our model as

$$\rho_{de} = \frac{3d_2^2\left(\left(2\,k+1\right)k_2\,t\right)^4}{8\pi d_1\left(3\,k_2\,t^2-12\,\frac{A_0}{k_2}\right)^4}\left(\left(1+\frac{\delta\pi\left(3\,k_2\,t^2-12\,\frac{A_0}{k_2}\right)^2}{\left(\left(2\,k+1\right)k_2\,t\right)^2}\right)^{\frac{d_1}{\delta}} - 1\right). \tag{35}$$

Using Eqs. (34), (27) and (26) in Eq. (15), we get the energy density of matter as

$$\begin{aligned}\rho_m \;=\; & \frac{\phi_0}{8\pi}\left(\frac{k_2\,t^2}{4}-\frac{A_0}{k_2}\right)^{\frac{n(2\,k+1)}{6}}\left\{\frac{2\,{k_2}^2t^2k}{\left(k_2\,t^2-4\,\frac{A_0}{k_2}\right)^2}+\frac{k^2{k_2}^2t^2}{\left(k_2\,t^2-4\,\frac{A_0}{k_2}\right)^2}-\left(\frac{k_2\,t^2}{4}-\frac{A_0}{k_2}\right)^{-1}\right.\\ & \left.-\frac{wn^2{k_2}^2\left(2\,k+1\right)^2t^2}{2\left(3\,k_2\,t^2-12\,\frac{A_0}{k_2}\right)^2}+nk_2\,\left(2\,k+1\right)t\left(\frac{k_2\,t+2\,kk_2\,t}{\left(k_2\,t^2-4\,\frac{A_0}{k_2}\right)}\right)\left(3\,k_2\,t^2-12\,\frac{A_0}{k_2}\right)^{-1}\right\}\\ & -\frac{3{d_2}^2\left(2\,k+1\right)^4{k_2}^4t^4}{\left(3\,k_2\,t^2-12\,\frac{A_0}{k_2}\right)^4 8\pi\,d_1}\left(\left(1+\frac{\delta\,\pi}{\left(2\,k+1\right)^2{k_2}^2t^2}\left(3\,k_2\,t^2-12\,\frac{A_0}{k_2}\right)^2\right)^{\frac{d_1}{\delta}}-1\right).\end{aligned} \tag{36}$$

Using Eqs. (34), (27) and (26), from Eq. (20) and (21) we obtain the EoS parameter of SMHDE as

$$\begin{aligned}\omega_{smhde} \;=\; & -\frac{\phi_0\,d_1}{3{d_2}^2\left(2\,k+1\right)^4{k_2}^4t^4}\left(\frac{k_2\,t^2}{4}-\frac{A_0}{k_2}\right)^{\frac{n(2\,k+1)}{6}}\left(3\,k_2\,t^2-12\,\frac{A_0}{k_2}\right)^4\left\{\frac{3k^2{k_2}^2t^2}{\left(\frac{k_2\,t^2}{4}-\frac{A_0}{k_2}\right)^2}\right.\\ & +\frac{3\,kk_2}{\left(k_2\,t^2-4\,\frac{A_0}{k_2}\right)}+\frac{16(k^2k_2^2t^2-kk_2{}^2t^2)-k_2^2t^2}{16\left(\frac{k_2\,t^2}{4}-\frac{A_0}{k_2}\right)^2}+\frac{k^2{k_2}^2t^2+kk_2^2t^2}{\left(k_2\,t^2-4\,\frac{A_0}{k_2}\right)^2}+\frac{wn^2{k_2}^2\left(2\,k+1\right)^2t^2}{\left(3\,k_2\,t^2-12\,\frac{A_0}{k_2}\right)^2}\\ & +\frac{n^2\left(2\,k+1\right)^2{k_2}^2t^2}{72\left(\frac{k_2\,t^2}{4}-\frac{A_0}{k_2}\right)^2}+\frac{2\,nk_2\,\left(2\,k+1\right)}{\left(3\,k_2\,t^2-12\,\frac{A_0}{k_2}\right)}-\frac{n\left(2\,k+1\right){k_2}^2t^2}{12\left(\frac{k_2\,t^2}{4}-\frac{A_0}{k_2}\right)^2}\\ & \left.+\left(\frac{(nk_2\,\left(2\,k+1\right)t)(k_2\,t+3\,kk_2\,t)}{3\left(k_2\,t^2-4\,\frac{A_0}{k_2}\right)^2}\right)\right\}\left(\left(1+\frac{\left(2\,k+1\right)^{-2}\delta\,\pi}{\left(3\,k_2\,t^2-12\,\frac{A_0}{k_2}\right)^{-2}{k_2}^2t^2}\right)^{\frac{d_1}{\delta}}-1\right)^{-1}.\end{aligned} \tag{37}$$

4. PHYSICAL DISCUSSION

This section examines the expansion of the universe by analyzing cosmological parameters such as the scalar field, EoS ω_{smhde}, squared sound speed v_s^2, deceleration q parameters, and the $\omega_{smhde}-\omega'_{smhde}$ plane for the anisotropic SMHDE model.

Scalar field: Figure 1 indicates the behavior of the scalar field in terms of cosmic time for various values of parameter k. The scalar field exhibits a positive value and experiences a steady decline throughout its development. The decreasing nature of the scalar field indicates the increasing pattern of kinetic energy in this model. Furthermore, we have seen that when the parameter k increases, the scalar field decreases.

EoS parameter: The equation of state parameter (ω) is often used for classifying the many phases of the expanding universe. The EoS parameter, represented as $\omega = \frac{p}{\rho}$, is a measure of the relationship between pressure (p) and energy density (ρ) of a given matter distribution. The decelerated and accelerated phases consist of the following time intervals: Decelerated phases, such as those involving cold dark matter or dust fluid (ω is zero), indicating the radiation era for (ω is between 0 and 1/3), and the fluid is characterized as stiff for $\omega = 1$. Accelerating phase, such as the cosmic constant/vacuum period (ω is -1), which corresponds to the quintessence period (when $-1 < \omega < -1/3$), it is known as the phantom era ($\omega < -1$), indicating a quintom period characterized by the mixture of both quintessence and phantom components.

The EoS parameter of SMHDE with Hubble horizon cutoff is given in Eq. (37). In Fig. 2, we investigate the evolution of EoS parameter ω_{smhde} in terms of cosmic time t for different values of k. Fig. 2 shows that initially ω_{smhde} starts from DE era, varies in quintessence region $-1 < \omega_{smhde} < -1/3$ and phantom region $\omega_{smhde} < -1$. As the parameter k increases the EoS parameter of our model enters into phantom region.

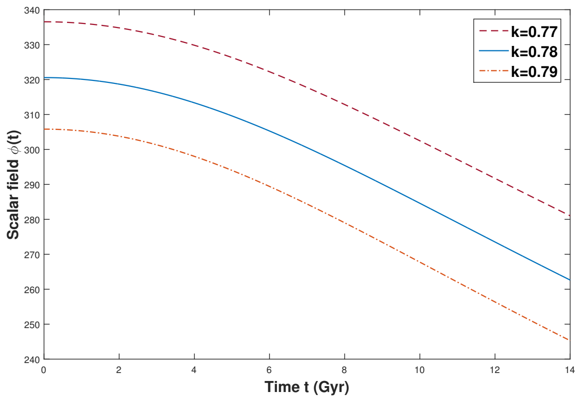

Figure 1. Plot of scalar field versus cosmic time t for $A_0 = -3900.69$ and $\phi_0 = 1750$.

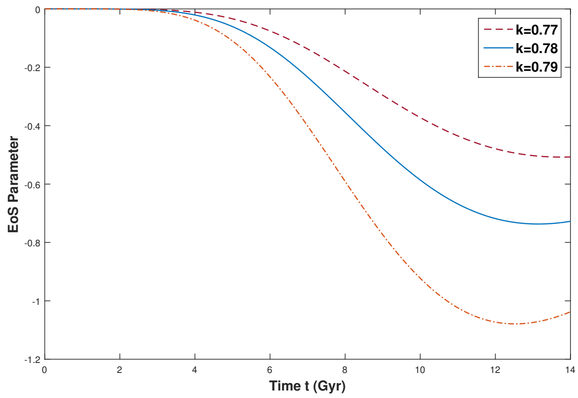

Figure 2. Plot of EoS parameter versus cosmic time t for $A_0 = -3900.69$, $\delta = 1.5$, $d_1 = 4.5$, $d_2 = 2.2$ and $\omega = 75000$.

Squared sound speed: The squared speed of the sound parameter is defined as

$$v_s^2 = \frac{\dot{p}_{smhde}}{\dot{\rho}_{smhde}} = \omega_{smhde} + \frac{\rho_{smhde}}{\dot{\rho}_{smhde}}\,\dot{\omega}_{smhde}. \tag{38}$$

The sign of this parameter is essential when considering the stability of DE models. The stability of the DE model is determined by the positive signature of v_s^2. If the signature is negative, the model becomes unstable. By substituting the energy density and EoS parameter from equations (35) and (37) into the equation for squared sound speed (v_s^2) provided by equation (38), we do a graphical analysis of v_s^2 for our model. Figure 2 illustrates the relationship between the square of the velocity, denoted as v_s^2, and the time t. The trajectories exhibit positive behaviour throughout the model's development. Therefore, this demonstrates the stability of our model.

$\omega_{smhde} - \omega'_{smhde}$ *plane:* We examine the $\omega_{smhde} - \omega'_{smhde}$ plane, where ω'_{smhde} represents the rate of change of the EoS parameter ω_{smhde} concerning the natural logarithm of the scale factor '*ln a*'. Caldwell and Linder [55] propose using this framework to examine the cosmic evolution of the quintessence DE scenario. Moreover, it has been observed that the $\omega_{smhde} - \omega'_{smhde}$ plane can be separated into two distinct areas: thawing ($\omega_{smhde} < 0$, $\omega'_{smhde} > 0$) and freezing ($\omega_{smhde} < 0$, $\omega'_{smhde} < 0$). The freezing zone exhibits a more accelerated phase of cosmic expansion in comparison to the thawing area.

Figure 4 depicts the relationship between the $\omega_{smhde} - \omega'_{smhde}$ plane and various values of k. Figure 4 demonstrates that the $\omega_{smhde} - \omega'_{smhde}$ plane represents the area where freezing occurs, regardless of the specific parameter values. Modern cosmological data suggest that the freezing zone exhibits a phase of increased cosmic acceleration in contrast to the thawing area. Hence, the $\omega_{smhde} - \omega'_{smhde}$ plane of our model exhibits cosmic acceleration inside the freezing region.

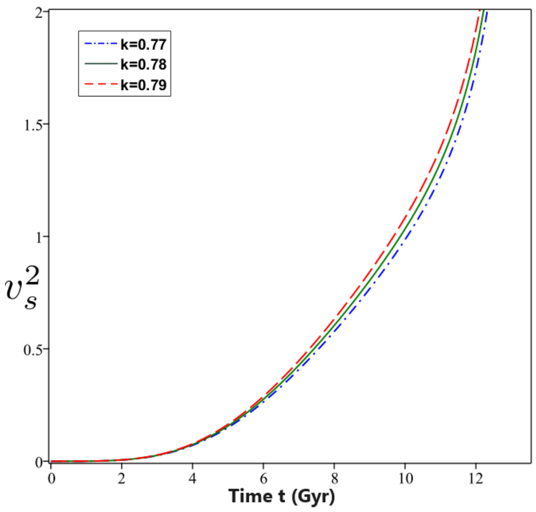

Figure 3. Plot of v_s^2 versus time t for $A_0 = -3900.69$, $\delta = 1.5$, $d_1 = 4.5$, $d_2 = 2.2$ and $\omega = 75000$.

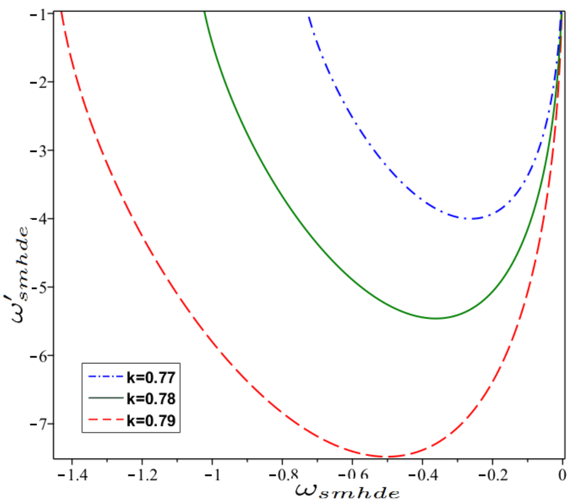

Figure 4. Plot of $\omega_{smhde} - \omega'_{smhde}$ for $A_0 = -3900.69$, $\delta = 1.5$, $d_1 = 4.5$, $d_2 = 2.2$ and $\omega = 75000$.

Energy conditions: The Raychaudhuri equations initiated the exploration of energy conditions, playing a crucial role in analyzing the alignment of null and time-like geodesics. The energy conditions are used to illustrate other universal principles about the dynamics of intense gravitational fields. The often observed energy conditions are as follows:

Dominant energy condition (DEC): $\rho_{smhde} \geq 0$, $\rho_{smhde} \pm p_{smhde} \geq 0$.

Strong energy conditions (SEC) : $\rho_{smhde} + p_{smhde} \geq 0$, $\rho_{smhde} + 3p_{smhde} \geq 0$,

Null energy conditions (NEC): $\rho_{smhde} + p_{smhde} \geq 0$,

Weak energy conditions (WEC): $\rho_{smhde} \geq 0$, $\rho_{smhde} + p_{smhde} \geq 0$,

Figure 5 illustrates the energy conditions of our SMHDE model. It is seen that the WEC satisfies the condition $\rho_{smhde} \geq 0$. Also, Fig. 5 demonstrates that the SEC $\rho_{smhde} + 3p_{smhde} \geq 0$ is not fulfilled. This phenomenon, resulting from the universe's acceleration in its latter stages, aligns with current observational findings.

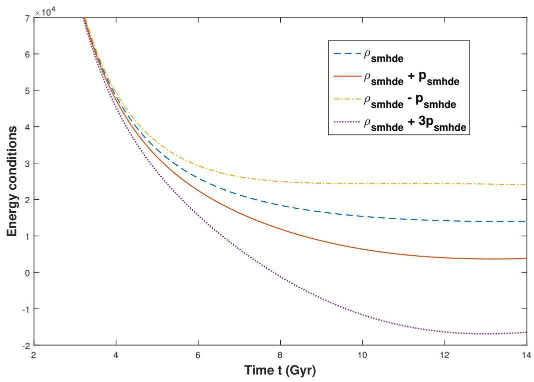

Figure 5. Plot of energy conditions versus cosmic time t for $A_0 = -3900.69$, $\delta = 1.5$, $d_1 = 4.5$, $d_2 = 2.2$ and $\omega = 75000$.

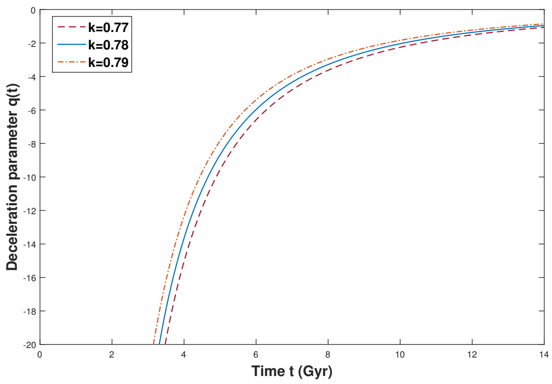

Figure 6. Plot of deceleration parameter versus cosmic time t for $A_0 = -3900.69$.

Deceleration parameter: The expansion of the universe may be determined by using the dimensionless cosmological parameter referred to as the deceleration parameter (DP). When DP has positive values, the model slows down in the usual manner. However, when q is equal to zero, the model grows at a consistent pace. The model demonstrates accelerated expansion when the value of q is between -1 and 0, and a super-exponential expansion when q is less than -1. Using Eqs. (11) and (30), we get the deceleration parameter can be calculated as

$$q=\frac{3\,{k_2}^2 t^2+12\,{A_0}^2}{(2\,k+1)\,{k_2}^2 t^2}-1. \tag{39}$$

Figure 5 displays the behavior of the deceleration parameter q in terms of cosmic time t for different values of k. It is important to mention that our model is accelerating throughout the evolution of the model and which is consistent with the recent observational data.

5. CONCLUSIONS

The accelerated expansion phenomenon of the universe has got much attraction with the passage of time. Upto now, many approaches have been adopted for explaining this phenomenon with variety of dynamical DE models and modified theories of gravity. Here, we reconsider the expansion phenomenon in the Brans-Dicke scenario leads to an accelerated universe. Thus, we have considered the Sharma-Mittal holographic dark energy within the context of anisotropic Bianchi type-VI_0 space-time in Brans-Dicke theory of gravitation. In this case, we have assumed the Hubble horizon as the infrared cutoff. We have examined well-recognized cosmological parameters, including the equation of state, deceleration, squared speed of sound parameters and $\omega_{smhde}-\omega'_{smhde}$ plane. Our findings have been condensed into the following summary:

The scalar field exhibits a positive value and experiences a steady decrease throughout its development. The decreasing nature of the scalar field indicates the increasing pattern of kinetic energy in this model. Furthermore, we have seen that when the parameter k increases, the scalar field decreases. The EoS parameter ω_{smhde} of the SMHDE model initially starts from the dark energy era and varies in quintessence region $-1<\omega_{smhde}<-1/3$ and finally it becomes less than -1, which means the model approaches phantom region at late times. We have made a comparison of our results with present Planck collaboration data [56] where the limits on the EoS parameter are given as $\omega_{de}=-1.56^{+0.60}_{-0.48}$ (Planck + TT + lowE), $\omega_{de}=-1.58^{+0.52}_{-0.41}$ (Planck + TT, TE, EE + lowE), $\omega_{de}=-1.57^{+0.50}_{-0.40}$ (Planck + TT, TE, EE + lowE + lensing), $\omega_{de}=-1.04^{+0.10}_{-0.10}$ (Planck + TT, TE, EE + lowE + lensing + BAO). It can be seen that the results for the EoS parameter of our model are consistent with the Planck Collaboration data. The $\omega_{smhde}-\omega'_{smhde}$ plane depicts the area where freezing occurs for all three parameter values. Modern cosmological measurements indicate that the freezing zone reveals a period of greater cosmic acceleration compared to the thawing region. Therefore, the $\omega_{smhde}-\omega'_{smhde}$ plane of our model demonstrates cosmic acceleration in the freezing area and aligns well with the facts. The paths of the $\omega_{smhde}-\omega'_{smhde}$ plane, as predicted by our model, align with the observed data [57, 58] $\omega_{smhde}=-1.13^{+0.24}_{-0.25}$, $\omega'_{smhde}<1.32$ (Planck+WP+BAO). The squared sound speed trajectories exhibit positive behaviour throughout the evolution of the universe and hence our model is stable. Our model violates the SEC regulations and this phenomenon resulting from the universe's acceleration in its latter epochs aligns with current observational data. Our model demonstrates an accelerating expansion of the universe throughout the evolution of model.

Acknowledgments

Y. Aditya is thankful to the National Board for Higher Mathematics, Department of Atomic Energy, Govt. of India for its financial support under the grant No: 02011/8/2023 NBHM(R.P.)/R & D II/3073.

ORCID

Y. Aditya, https://orcid.org/0000-0002-5468-9697; **D. Tejeswararao**, https://orcid.org/0000-0003-3508-346X; **U.Y. Divya Prasanthi**, https://orcid.org/0009-0004-5397-050X

REFERENCES

[1] S. Perlmutter, et al., Astrophys. J. **517**, 565 (1999). https://doi.org/10.1086/307221

[2] A.G. Riess, et al., Astron. J. **116**, 1009 (1998). https://doi.org/10.1086/300499

[3] T. Koivisto, and D.F. Mota, Phys. Rev. D, **73**, 083502 (2006). https://doi.org/10.1103/PhysRevD.73.083502

[4] E.J. Copeland, et al., Int. J. Mod. Phys. D, **15**, 1753 (2006). https://doi.org/10.1142/S021827180600942X

[5] R.R. Caldwell, and M. Kamionkowski, Ann. Rev. Nucl. Part. Sci. **59**, 397 (2009). https://doi.org/10.1146/annurev-nucl-010709-151330

[6] K. Bamba, et al., Astrophys. Space Sci. **342**, 155 (2012). https://doi.org/10.1007/s10509-012-1181-8

[7] S. Nojiri, et al., Phys. Rept. **692**, 1 (2017). https://doi.org/10.1016/j.physrep.2017.06.001

[8] Q.G. Huang, M. Li, J. Cosmol. Astropart. Phys. **3**, 1 (2005). https://doi.org/10.1088/1475-7516/2004/08/013

[9] M. Li, Phys. Lett. B, **603**, 1 (2004). https://doi.org/10.1016/j.physletb.2004.10.014

[10] A. Cohen, and D. Kaplan, A. Nelson, Phys. Rev. Lett. **82**, 4971 (1999). https://doi.org/10.1103/PhysRevLett.82.4971
[11] L.N. Granda, and A. Oliveros, Phys. Lett. B, **671**, 199 (2009). https://doi.org/10.1016/j.physletb.2008.12.025
[12] H. Wei, and R.G. Cai, Phys. Lett. B, **660**, 113 (2008). https://doi.org/10.1016/j.physletb.2007.12.030
[13] S. Nojiri, and S.D. Odintsov, Gen. Rel. Grav. **38**, 1285 (2006). https://doi.org/10.1007/s10714-006-0301-6
[14] S. Nojiri, et al., Phys. Lett. B, **797**, 134829 (2019). https://doi.org/10.1016/j.physletb.2019.134829
[15] M. Tavayef, A. Sheykhi, K. Bamba, and H. Moradpour, Phys. Lett. B, **781**, 195 (2018). https://doi.org/10.1016/j.physletb.2018.04.001
[16] C. Tsallis, and L.J.L. Cirto, Eur. Phys. J. C, **73**, 2487 (2013). https://doi.org/10.1140/epjc/s10052-013-2487-6
[17] A.S. Jahromi et al., Phys. Lett. B, **780**, 21 (2018). https://doi.org/10.1016/j.physletb.2018.02.052
[18] H. Moradpour et al., Eur. Phys. J. C, **78**, 829 (2018). https://doi.org/10.1140/epjc/s10052-018-6309-8
[19] D.R.K. Reddy, et al., Astrophys Space Sci. **361**, 356 (2016). https://doi.org/10.1007/s10509-016-2938-2
[20] Y. Aditya, and D.R.K. Reddy, Eur. Phys. J. C, **78**, 619 (2018). https://doi.org/10.1140/epjc/s10052-018-6074-8
[21] V.U.M. Rao, et al., Results in Physics, **10**, 469 (2018). https://doi.org/10.1016/j.rinp.2018.06.027
[22] M.V. Santhi, et al., Int. J. Theor. Phys. **56**, 362 (2017). https://doi.org/10.1007/s10773-016-3175-8
[23] K.D. Naidu, et al., Eur. Phys. J. Plus, **133**, 303 (2018). https://doi.org/10.1140/epjp/i2018-12139-2
[24] Y. Aditya, et al., Eur. Phys. J. C, **79**, 1020 (2019). https://doi.org/10.1140/epjc/s10052-019-7534-5
[25] S. Maity, U. Debnath, Eur. Phys. J. Plus, **134**, 514 (2019). https://doi.org/10.1140/epjp/i2019-12884-6
[26] A. Iqbal, A. Jawad, Physics of the Dark Universe, **26**, 100349 (2019). https://doi.org/10.1016/j.dark.2019.100349
[27] G. Kaniadakis, Physica A: Stat. Mech. and its Appl. **296**(3-4), 405 (2001). https://doi.org/10.1016/S0378-4371(01)00184-4
[28] M. Masi, Phys. Lett. A, **338**, 217 (2005). https://doi.org/10.1016/j.physleta.2005.01.094
[29] E.M. Abreu, et al., EPL (Europhysics Letters), **124**, 30003 (2018). https://doi.org/10.1209/0295-5075/124/30003
[30] H. Moradpour, et al. Eur. Phys. J. C, **80**, 1 (2020). https://doi.org/10.1140/epjc/s10052-020-8307-x
[31] A. Jawad, and A.M. Sultan, Adv. High Energy Phys. **2021**, 5519028 (2021). https://doi.org/10.1155/2021/5519028
[32] U.K. Sharma, et al., IJMPD, **31**, 2250013 (2022). https://doi.org/10.1142/S0218271822500134
[33] N. Drepanou et al., ur. Phys. J. C, **82**, 449 (2022). https://doi.org/10.1140/epjc/s10052-022-10415-9
[34] J. Sadeghi, et al., arXiv:2203.04375 (2022). https://doi.org/10.48550/arXiv.2203.04375
[35] O. Akarsu, and C.B. Kilinc, Astrophys. Space Sci. **326**, 315 (2010). https://doi.org/10.1007/s10509-009-0254-9
[36] C.L. Bennett, et al., Astron. Astrophys. Suppl. Ser. **148**, 1 (2003). https://doi.org/10.1086/377252
[37] D.R.K. Reddy, et al., Can. J. Phys. **97**, 932 (2019). https://doi.org/10.1139/cjp-2018-0403
[38] Y. Aditya, et al., Astrophys. Space Sci. **364**, 190 (2019). https://doi.org/10.1007/s10509-019-3681-2
[39] Y. Aditya, and D.R.K. Reddy, Astrophys. Space Sci. **364**, 3 (2019). https://doi.org/10.1007/s10509-018-3491-y
[40] Y. Aditya, et al., Ind. J. Phys. **95**, 383 (2021). https://doi.org/10.1007/s12648-020-01722-6
[41] R.L. Naidu, et al., Astrophys. Space Sci. **365**, 91 (2020). https://doi.org/10.1007/s10509-020-03796-4
[42] K.D. Naidu, et al., Mod. Phys. A, **36**, 2150054 (2021). https://dx.doi.org/10.1142/S0217732321500541
[43] Y. Aditya, et al., New Astr. **84**, 101504 (2021). https://doi.org/10.1016/j.newast.2020.101504
[44] Y. Aditya, et al., Int. J. Mod. Phys. A, **37**, 2250107 (2022). https://doi.org/10.1142/S0217751X2250107X
[45] M.P.V.V. Bhaskara Rao, et al., New Astr. **92**, 101733 (2022). https://doi.org/10.1016/j.newast.2021.101733
[46] U.Y.D. Prasanthi, and Y. Aditya, Phys. Dark Univ. **31**, 100782 (2021). https://doi.org/10.1016/j.dark.2021.100782
[47] U.Y.D. Prasanthi, and Y. Aditya, Results Phys. **17**, 103101 (2020). https://doi.org/10.1016/j.rinp.2020.103101
[48] Y. Aditya, and U.Y.D. Prasanthi, Bulg. Astr. Journal, **38**, 52 (2023). https://astro.bas.bg/AIJ/issues/n38/YAditya.pdf
[49] Y. Aditya, Bulg. Astr. Journal, **39**, 12 (2023). https://astro.bas.bg/AIJ/issues/n39/YAditya.pdf
[50] C.H. Brans, R.H. Dicke, Phys. Rev. **124**, 925 (1961). https://doi.org/10.1103/PhysRev.124.925
[51] C.B. Collins, et al., Gen. Relativ. Gravit. **12**, 805 (1980). https://doi.org/10.1007/BF00763057

[52] V.B. Johri, R. Sudharsan, Australian J. of Phys. **42(2)**, 215 – 222 (1989). https://doi.org/10.1071/PH890215

[53] V.B. Johri, K. Desikan, Gen Relat Gravit **26**, 1217–1232 (1994). http://dx.doi.org/10.1007/BF02106714

[54] B.D. Sharma, D.P. Mittal, J. Math. Sci. **10**, 28 (1975).

[55] R. Caldwell, and E.V. Linder, Phys. Rev. Lett. **95**, 141301 (2005). https://doi.org/10.1103/PhysRevLett.95.141301

[56] N. Aghanim, et al., [Plancks Collaboration] arXiv:1807.06209v2 (2018). https://doi.org/10.48550/arXiv.1807.06209

[57] P.A.R. Ade, et al., Astrophys. **571**, A16 (2014). https://doi.org/10.1051/0004-6361/201321591

[58] G.F. Hinshaw, et al., Astrophys. J. Suppl. **208**, 19 (2018). https://doi.org/10.1088/0067-0049/208/2/19

КОСМІЧНІ АСПЕКТИ ГОЛОГРАФІЧНОЇ МОДЕЛІ ТЕМНОЇ ЕНЕРГІЇ ШАРМА-МІТТАЛА В ТЕОРІЇ ГРАВІТАЦІЇ БРЕНСА-ДІККЕ

Ю. Адітья[a], Д. Теджешварарао[a], У.Ю. Дів'я Прасанті[b]

[a] *Департамент фундаментальних та гуманітарних наук, Технологічний інститут GMR, Раджам-532127, Індія*

[b] *Факультет статистики та математики Коледжу садівництва, Університет рослинництва Dr.Y.S.R., Парватипурам-535502, Індія*

Ми досліджуємо космологічний сценарій із просторово однорідним і анізотропним простором-часом типу Б'янкі VI_0 в контексті голографічної моделі темної енергії Шарма-Міттала в рамках теорії гравітації Бранса-Дікке. Для досягнення цієї мети обговорювалися Хаббл, уповільнення, параметри рівняння стану. Параметр уповільнення (q) використовується для вимірювання темпу, з яким прискорюється розширення Всесвіту. Параметр рівняння стану (ω_{smhde}) характеризує квінтесенцію та вакуумні області Всесвіту. Усі параметри демонструють узгоджену поведінку відповідно до даних Planck 2018. Ми оцінюємо динамічну стабільність, визначаючи квадрат швидкості звуку та досліджуючи його поведінку. Крім того, енергетичні умови та варіація ω_{smhde} і ω'_{smhde} у моделі вказують на поточне прискорене розширення Всесвіту.

Ключові слова: *модель типу Bianchi-VI_0; модель темної енергії; теорія гравітації Бренса-Дікке; космологія; голографічна темна енергія Шарма-Міттала*